Determining the Activation Time Course of Synaptic AMPA Receptors from Openings of Colocalized NMDA Receptors

Ingo C. Kleppe and Hugh P. C. Robinson
Physiological Laboratory, University of Cambridge, Downing St., Cambridge CB2 3EG, United Kingdom

ABSTRACT Excitatory postsynaptic currents (EPSCs) in most mammalian central neurons have a fast α-amino-3-hydroxy-5-methyl-4-isoazole-proprionic acid (AMPA) receptor-mediated component, lasting a few milliseconds, and a slow *N*-methyl-D-aspartic acid (NMDA)-receptor-mediated component, lasting hundreds of milliseconds. The time course of the AMPA phase is crucial in the integrative function of neurons, but measuring it accurately is often confounded by cable filtering between the recording electrode and the synapse. We describe a method for recovering the AMPA phase of individual EPSCs by determining the impulse response of the cable filter from single NMDA channel transitions in the slow tails of the same EPSC, then deconvolving the measured AMPA current. Using simulations, we show that filtering of an AMPA conductance transient in a voltage-clamped dendrite behaves in an almost perfectly linear fashion. Expressions are derived for the time course of single channel transitions and the AMPA phase filtered through a voltage-clamped cable or a single exponential filter, using a kinetic model for AMPA receptor activation. Fitting these expressions to experimental records directly estimates the underlying kinetics of the AMPA phase. Example measurements of spontaneous EPSCs in cultured nonpyramidal rat cortical neurons yielded rising time constants of 0.2–0.8 ms, and decay time constants of 1.3–2 ms at 23–25°C.

INTRODUCTION

Most fast excitatory synapses in the mammalian central nervous system have two types of postsynaptic glutamate receptor channel: the α-amino-3-hydroxy-5-methyl-4-isoazole-proprionic acid (AMPA) receptor and the *N*-methyl-D-aspartic acid (NMDA) receptor (Ozawa et al., 1998). AMPA and NMDA receptor channels are localized together at synapses (Bekkers and Stevens, 1989; He et al., 1998), and presumably experience the same pulse of glutamate release from the presynaptic terminal. However, their time course of activation is very different. At room temperature, AMPA receptors activate and deactivate within a few milliseconds of presynaptic glutamate release, whereas the open probability of NMDA receptors typically reaches a peak after 20–30 ms, and decays over hundreds of milliseconds (Forsythe and Westbrook, 1988; Stern et al., 1992), the difference resulting from the lower affinity of AMPA receptors for glutamate. Therefore, voltage-clamped glutamate excitatory postsynaptic currents (EPSCs) appear biphasic, with a very fast AMPA transient, and a much slower NMDA tail.

The transient of conductance mediated by synaptic AMPA receptors is the major fast excitatory input to a mammalian central neuron. To know the exact size and timing of this transient is fundamentally important for understanding the mechanism of the excitatory synapse, and for understanding how neurons integrate their synaptic input. The timing of AMPA receptor activation at the synapse is expected to vary considerably, since native AMPA receptors are assembled as heteromers of four different subunits, each of which can occur in "flip" and "flop" splice variants, and which show different kinetics (Jonas et al., 1994; Mosbacher et al., 1994). The subunit composition of native AMPA receptors varies widely (Hollman and Heinemann, 1994; Ozawa et al., 1998).

However, the rapid time course of the AMPA phase and the dendritic location of the synapse mean that, in many cell types, it is heavily distorted and attenuated by the intervening dendritic cable when recorded by voltage-clamp at the soma. Approaches that have been taken to estimate the true kinetics of the fast AMPA phase have included detailed modeling of dendritic trees to simulate the effect of cable filtering (Spruston et al., 1993); use of voltage steps applied at different offsets in time during an ensemble of synaptic currents, to map out the time course of the underlying conductance change (Pearce, 1993; Häusser and Roth, 1997) and direct dendritic recording (Häusser, 1994).

Here, we develop a different approach to this problem. We have demonstrated previously that, in low-noise whole-cell recordings, the opening and closing transitions of single NMDA channels can be readily resolved in the tails of biphasic EPSCs, and we noted that, since these transitions are essentially perfect steps of current at the synaptic site, their time course measured at the soma can be used to estimate the cable filter (Robinson et al., 1991; see also Silver et al., 1995). If the cable filter is linear, then the AMPA phase from the same synaptic site is filtered in exactly the same way, and its true time course could be reconstructed by removing, or deconvolving, the effects of the cable filter from the measured records. This approach would have the potential to improve upon previous methods in both accuracy and ease of application. In this paper, we show that the assumption of linearity of the cable filter is a very good one for physiological cable parameters and cur-

Received for publication 7 April 1999 and in final form 7 June 1999.

Address reprint requests to Dr. Hugh Robinson, Physiological Laboratory, University of Cambridge, Downing St., Cambridge CB2 3EG, U.K., Tel.: +44-1223-333828; Fax: +44-1223-333840; E-mail: hpcr@cus.cam.ac.uk.

0006-3495/99/09/1418/10 $2.00

rent amplitudes. We find expressions to fit cable-filtered NMDA channel openings and AMPA phase currents for two cases: for a voltage-clamped uniform cable dendrite, and for the simpler case when filtering is approximated by a single exponential. We apply the latter theory to some example data from cultured rat cortical neurons.

MATERIALS AND METHODS

Cable simulations

For the simulations, a compartmental model of a voltage-clamped, one-dimensional uniform cable was constructed (see Figs. 1 and A2). Each compartment consisted of the resistance and capacitance of a length of cable which was one twentieth of a space constant (λ). The total length of the model was 10λ (200 compartments). The cable parameters were set to the middle of the ranges reported by Major et al., (1994): intracellular resistivity (R_i) was 250 Ω·cm, membrane capacitance (C_m) was 0.75 μF/cm^2, and membrane resistance (R_m) was 160 kΩ·cm^2. The potential at one end of the open cable was set to zero (short-circuit), while the other end was closed. The system of ordinary differential equations representing the cable was integrated using a variable order Adams–Bashforth–Moulton solver (ODE113, MATLAB, MathWorks, Natick, MA). The integral in Eq. 7 was evaluated by an adaptive recursive Newton Cotes quadrature method (QUAD8, MATLAB).

Recording

Primary dissociated cultures of rat cortex were prepared as described by Maeda et al., (1995) and maintained for 1–3 weeks before recording. Recordings of spontaneous synaptic currents were carried out in a bath solution with a composition of (mM): 140 NaCl, 2 $CaCl_2$, 10 glucose, 10 *N*-2-hydroxyethylpiperazine-*N*′-2-ethanesulfonic acid (HEPES), 3 KCl, 0.003 glycine, balanced to a pH of 7.35 with NaOH. The patch electrode solution contained (concentrations in mM): 100 Cs methanesulfonate, 0.3 GTP, 4 ATP, 20 CsCl, 10 HEPES/Na (pH 7.3), 20 phosphocreatine (Na_2), and 5 U/mL creatine phosphatase. Whole-cell voltage clamp recordings were carried out between days 8 and 21 of culture at room temperature (23–25°C) using an Axopatch 200A patch-clamp amplifier (Axon Instruments, Foster, CA). No series resistance correction was used to avoid introducing additional complexity to the cable filter function. The current signal was sampled at 10 kHz with 12-bit resolution, after filtering by a 2-kHz (−3 dB) cutoff 4-pole Bessel low-pass filter. The step response of the recording system was measured by applying a triangular wave of voltage to the speed test input of the Axopatch 200A, capacitatively inducing a square wave current input at the headstage.

Data analysis

Biphasic EPSCs were selected for analysis if they were well separated from any previous event. For each EPSC, clearly identifiable single NMDA channel opening and closing transitions were selected. The starting points of transitions were defined as the positions of maxima (closing) or minima (opening) in the derivatives of the records after smoothing with a Gaussian filter (Colquhoun and Sigworth, 1995), with corner frequencies between 1 and 2 kHz. Single exponentials were then fitted to the transitions by least-squares. The average time constant of these exponentials over the collection of 2–10 transitions in one biphasic event was taken as the filter time constant τ_f for the previous fast AMPA phase. AMPA phases were fitted by least-squares to Eq. 8, with five free parameters: A, τ_r, τ_d, the baseline level, and the time of initiation of the event.

RESULTS

Figure 1 demonstrates the severe effect of cable filtering on the kinetics of the fast, AMPA-receptor-mediated phase of the glutamatergic synaptic current. We calculated the current measured by a perfect voltage-clamp applied at one end of a long (effectively infinite) dendrite, of 2-μm diameter, using cable parameters in the middle of the ranges reported by Major et al. (1994)—to our knowledge, the most detailed study of the cable properties of a mammalian central neuron (see Materials and Methods). The form of the AMPA conductance transient was specified as the difference of two exponentials, as described in Appendix A, with a rising time constant of 0.5 ms, and a decay time constant of 2 ms, similar to the fastest values reported in the literature (Häusser & Roth, 1997; Silver et al., 1992; Hestrin, 1993; Forsythe & Barnes-Davies, 1993), and to the deactivation

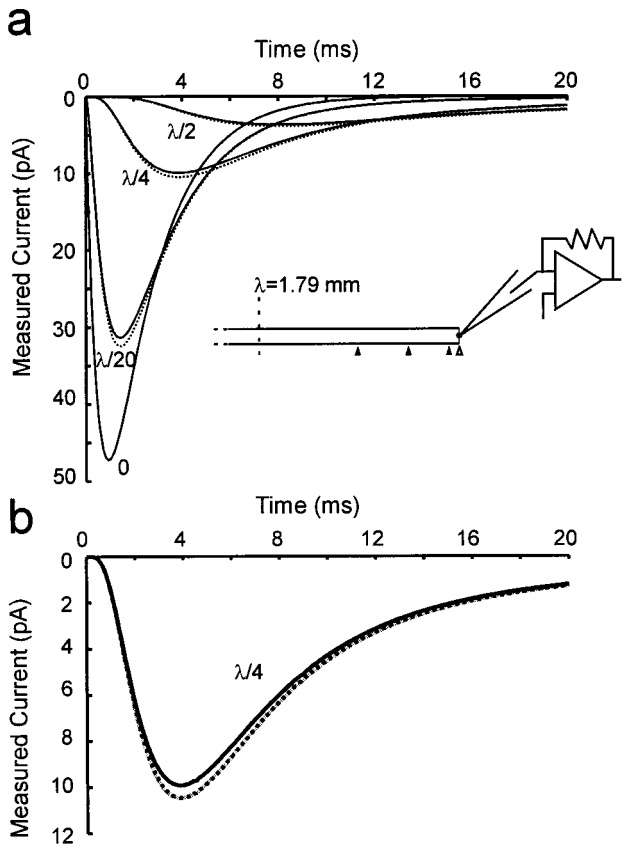

FIGURE 1 Cable filtering of AMPA conductance and current inputs in dendrites during voltage-clamp. (*a*) A numerical model of a semi-infinite dendrite, voltage-clamped at its origin, was constructed (*inset*, see Methods). The diameter of the dendrite was 2 μm, λ was 1.789 mm, and τ_m was 120 ms. *Solid curves:* voltage-clamp current during injection of an AMPA conductance transient $g(t) = \bar{g}(\exp(-t/\tau_2) - \exp(-t/\tau_1))$, which resulted in a current $I(t) = \bar{g}(\exp(-t/\tau_2) - \exp(-t/\tau_1))(V - E_{rev})$. E_{rev} was 60 mV positive to rest, $\bar{g}$ = 1.666 ns, τ_2 = 2 ms, τ_1 = 0.5 ms. *Dotted curves:* voltage-clamp currents during injection of a fixed current transient, $I(t) = \bar{g}E_{rev}(\exp(-t/\tau_2 - \exp(-t/\tau_1))$. Measured currents were slightly larger than those for conductance inputs, because of the reduction in driving force in the latter case, as the synaptic site depolarizes. At distance 0, the measured current is the same as that injected for both current and conductance injection. (*b*) Voltage-clamped dendrite behaves as a linear filter for conductance inputs. The conductance response at λ/4 (*solid curve*), scaled up by a factor of 1.0553 (*grey curve*) can be exactly superimposed on the current response (*dotted curve*).

kinetics of isolated AMPA receptors in fast perfusion experiments (Colquhoun et al., 1992). The measured current has the same shape as the underlying conductance when the synapse is located at the site of the voltage-clamp. As the synaptic input is moved away from the point of voltage-clamp, the measured current (*solid lines*) is slowed and diminished in amplitude. At $\lambda/20$ (90 μm), the measured current is slowed by about 25%; at $\lambda/4$ (448 μm), a situation similar to somatic recording of a distal input to a cortical pyramidal neuron, the apparent kinetics are slowed by more than a factor of 4. The distortion is worse in dendrites of smaller diameter.

This cable filtering effect has been documented in a number of studies (for example, Carnevale and Johnston, 1982; Johnston and Brown, 1983; Spruston et al., 1993), and means that the true time course of the AMPA phase is usually much faster than that recorded.

In Fig. 1 *a*, we also plot the current measured by the voltage-clamp (*dotted lines*) for current inputs of the same time course: that is, the current that would be produced by the conductance transient if there were no voltage excursion at the synaptic site. Making this assumption introduces a small error, of about 5%, in the peak amplitude, which remains almost constant over the range of distances shown. More importantly, however, the normalized time courses of the conductance and current responses are virtually identical: scaling up the conductance response allows it to be superimposed exactly on the current response over its entire time course (Fig. 1 *b*). This was confirmed for distances up to λ and for the entire range of cable parameters quoted in Major et al. (1994): $C_m = 0.7–0.8$ μF/cm^2; $R_i = 170–340$ Ω·cm; $R_m = 120–200$ kΩ·cm^2 (see Materials and Methods). The very close correspondence between measured time courses for conductance and current input only breaks down for unrealistically high amplitudes of conductance.

Therefore, in practice, the current measured in response to a transient conductance input in a voltage-clamped dendrite, held within its passive range of response, has the same time course as that measured for the equivalent current input. This allows us to consider the voltage-clamped dendrite as a linear cable filter of the synaptic input. We may write the measured voltage-clamp current, $I_{VC}(t)$, as

$$I_{VC}(t) = F * I_{syn}(t), \tag{1}$$

where F is the impulse response of the filter (a combination of the cable filter and filtering by the measurement apparatus), $I_{syn}(t)$ is the synaptic current waveform, and $*$ denotes convolution. Thus, knowing I_{VC} and F, it is possible to recover I_{syn} by deconvolution.

F may be estimated independently as follows. As pointed out in Robinson et al. (1991), single NMDA channel transitions resolved in the whole-cell synaptic current represent effectively perfect step current inputs at the same synaptic site as the AMPA phase. Opening and closing transitions of ionic channels are too fast to distinguish from the step response of patch-clamp recording systems, but are believed to happen within a few μs or less (Sigworth, 1986; Hille, 1992). Each transition, therefore, is a scaled version of the step response of the combined cable and apparatus filter. Since the filter can be taken to be linear, the measured AMPA phase current is given by

$$I_{VC}(t) = \left(\frac{I'_{NMDA}}{i_{NMDA}}\right) * I_{AMPA}, \tag{2}$$

where $I'_{NMDA}(t)$ is the first derivative of the time course of the opening transition of an NMDA channel, and i_{NMDA} is the single NMDA channel amplitude (the impulse response is the first derivative of the step response). This equation shows how the true kinetics of the AMPA phase may be recovered from cable-filtered biphasic synaptic events if single channel transitions can be resolved in the NMDA phase. In general, any method of numerical deconvolution may be used: for example, dividing the fast Fourier transform of I_{VC} by that of $I'_{NMDA}(t)/i_{NMDA}$ and taking the inverse fast Fourier transform. The filtering effect of the recording apparatus does not need to be distinguished from the cable filter to calculate the true AMPA phase time course. If an estimate of the cable filter (F_{cable}) alone is required, the combined filter can be deconvolved with the known impulse response of the apparatus filter (F_{app}), since

$$F = F_{app} * F_{cable}. \tag{3}$$

From Eq. 2, if a value for i_{NMDA} at the synaptic site is known, then deconvolution gives the correct amplitude of $I_{AMPA}(t)$. If unknown, i_{NMDA} can be assumed to be the same as that for extrasynaptic NMDA receptors, or estimated as described below. However, i_{NMDA} is simply a scaling factor and has no influence on measurements of the kinetics. If this numerical deconvolution approach is used, several single-channel transitions should be averaged, and a smooth function fitted to their time course to minimize the effect of noise on the reconstructed AMPA phase.

An alternative approach is to derive an analytical expression for the measured current, assuming a particular form for the underlying AMPA conductance transient and for the cable filter. For this purpose, we used a two-exponential description of the AMPA phase current,

$$I(t) = A(e^{-k_2 t} - e^{-k_1 t}), \tag{4}$$

where k_1 is the activation rate constant, k_2 is the decay rate constant, and A is a scaling constant. This empirical approximation was accurate enough to produce good fits to the recorded AMPA phases, as will be seen below.

In Appendix A, the impulse and step responses of a voltage-clamped infinite uniform cable are derived as a model for a dendrite or an equivalent cylinder representation of a branching dendritic tree. The impulse response is given by

$$I(T) = \frac{Q_0 L \exp[(-L^2 - 4T^2)/4T]}{2\tau_m \sqrt{\pi} T^{3/2}}, \tag{5}$$

in which Q_0 is the amount of charge injected as an impulse, λ is the space constant of the cable, L is the distance between the site of charge injection and the point of voltage-clamp in units of λ, τ_m is the membrane time constant, and T is time in units of τ_m. The step response is given by

$$I(T) = \frac{I_0}{2}\left\{e^{-L} + e^{-L}\mathrm{erf}\left(\frac{2T - L}{2\sqrt{T}}\right) + e^{L}\mathrm{erfc}\left(\frac{2T + L}{2\sqrt{T}}\right)\right\}, \quad (6)$$

where I_0 is the size of the step current input. We then obtained an expression for the cable-filtered current, by convolving Eqs. 4 and 5,

$$I(T) = \frac{LA}{2\sqrt{\pi}}\int_0^T \frac{\exp(k_1u - k_1T) - \exp(k_2u - k_2T)}{u^{3/2}\exp(u + (L^2/4u))}\,du. \quad (7)$$

To recover the rate constants and amplitude of an AMPA phase current, one first fits the accompanying opening and closing transitions of NMDA channels to Eq. 6, with I_0 ($= i_{NMDA}$) and L as free parameters. The value of L obtained in this way is then used to fit the AMPA phase using Eq. 7 with k_1, k_2, and A as free parameters. The membrane time constant, τ_m, could be measured independently from the charging transients of the cell (Rall, 1969; Jackson, 1992), or could be treated as an additional free parameter of the fit.

We studied the performance of this procedure in estimating the shape and size of the AMPA phase using synthetic data generated for a range of values of L, the synaptic distance. As seen in Fig. 2 *b*, both i_{NMDA} and L are estimated very accurately, from even a few single channel transitions, over the range of L investigated (up to $\lambda/2$). k_1, k_2, and A are then estimated by fitting the AMPA phase with Eq. 7 using the values of L obtained from the single channel fits. As shown in Fig. 2 *c*, all three parameters can be estimated accurately under realistic conditions, with no systematic error in the means, as L is increased. The standard deviation of the fits increases with L as the size of event is attenuated relative to the baseline noise level. Not surprisingly, estimates of k_1 have the largest standard deviation, because they are mostly determined by the very short-lived rising phase of the AMPA current.

To apply this method of fitting a cable-filtered kinetic equation to records, the filtering effect of the recording apparatus (the voltage-clamp amplifier and any analog or digital filtering applied to the data) should also be considered. There are three ways to treat it. First, it could be ignored if its step response is fast enough. Second, it could be removed by deconvolving records from the measured impulse response of the recording system before analysis. Third, Eq. 7 could be further convolved with an analytical expression for the apparatus impulse response by, for example, using the Laplace transforms given in Appendix A.

A simpler expression than given above results from assuming the same form of current input, but treating the lumped cable and apparatus filter as having a single exponential impulse (or step) response, of time constant τ_f (Appendix B). The form of the observed AMPA current should then be

$$I(t) = AD\left[\frac{\tau_d\exp(-t/\tau_d)}{\tau_d - \tau_f} - \frac{\tau_r\exp(-t/\tau_r)}{\tau_r - \tau_f} + \frac{\tau_f(\tau_d - \tau_r)\exp(-t/\tau_f)}{(\tau_f - \tau_d)(\tau_f - \tau_r)}\right], \quad (8)$$

where the decay time constant, τ_d, is $1/k_2$, the rising time constant, τ_r, is $1/k_1$, and D is the ratio of observed to actual i_{NMDA} (i.e., the scaling factor of the exponential filter).

This expression was applied to spontaneously occurring biphasic EPSCs, recorded in small, nonpyramidal cultured rat cortical neurons. Whole-cell recording was carried out in nominally zero magnesium external solution to free NMDA receptor channels from magnesium block (Nowak et al., 1984). At a holding potential of −60 mV, spontaneous EPSCs could be resolved as a sharp initial AMPA receptor-mediated phase followed by a long-lasting burst of NMDA channel openings (Fig. 3). After filtering with a Gaussian digital filter, individual NMDA channel openings were fitted with single exponential time courses (Fig. 4 *a*) as described in the Materials and Methods. The ensemble average of 12 opening transitions closely followed a single exponential, as illustrated by the log-linear plot in Fig. 4 *b*. Thus, practically, in these recordings, the exponential encapsulates the combined effects of cable and apparatus filtering well. This observation, which agrees with Silver et al. (1995), motivated the derivation of Eq. 8.

The time constants fitted to individual NMDA channel opening transitions were usually significantly slower than the step response of the recording system (Fig. 5 *a*). In one cell, time constants were distributed from 200 μs to over 5 ms, as shown in Fig. 5 *b*. Thus, for most NMDA channel transitions, cable filtering is a much larger distortion than instrumental filtering, and it varies over a wide range.

In practice, values for several (2–10) transitions were averaged together to estimate τ_f for each AMPA phase. The AMPA phase was then fitted with Eq. 8. Fits for two example AMPA phases from the same cell, but experiencing different degrees of cable filtering, are shown in Fig. 6. The underlying kinetics, however, were similar with τ_r values of 0.6 and 0.7 ms, and τ_d values of 1.5 and 1.7 ms, for Fig. 6, *a* and *b*, respectively. In three cells fitting a total of 51 AMPA phases, values of τ_r were in the range of 0.2–0.8 ms and τ_d in the range 1.2–2.35 ms. The average value of τ_r was 0.40 ± 0.23 ms, and the average value of τ_d was 1.50 ± 0.43 ms (mean ± SD). Errors in the fitting process were assessed from fitting synthetic data, in a way analogous to that shown in Fig. 2, and were much smaller than the observed standard deviations—below 0.1 ms SD for both τ_r and τ_d over the range of τ_f (not shown).

DISCUSSION

In this study, it is demonstrated that the distorting effect of measuring a fast synaptic conductance transient, separated

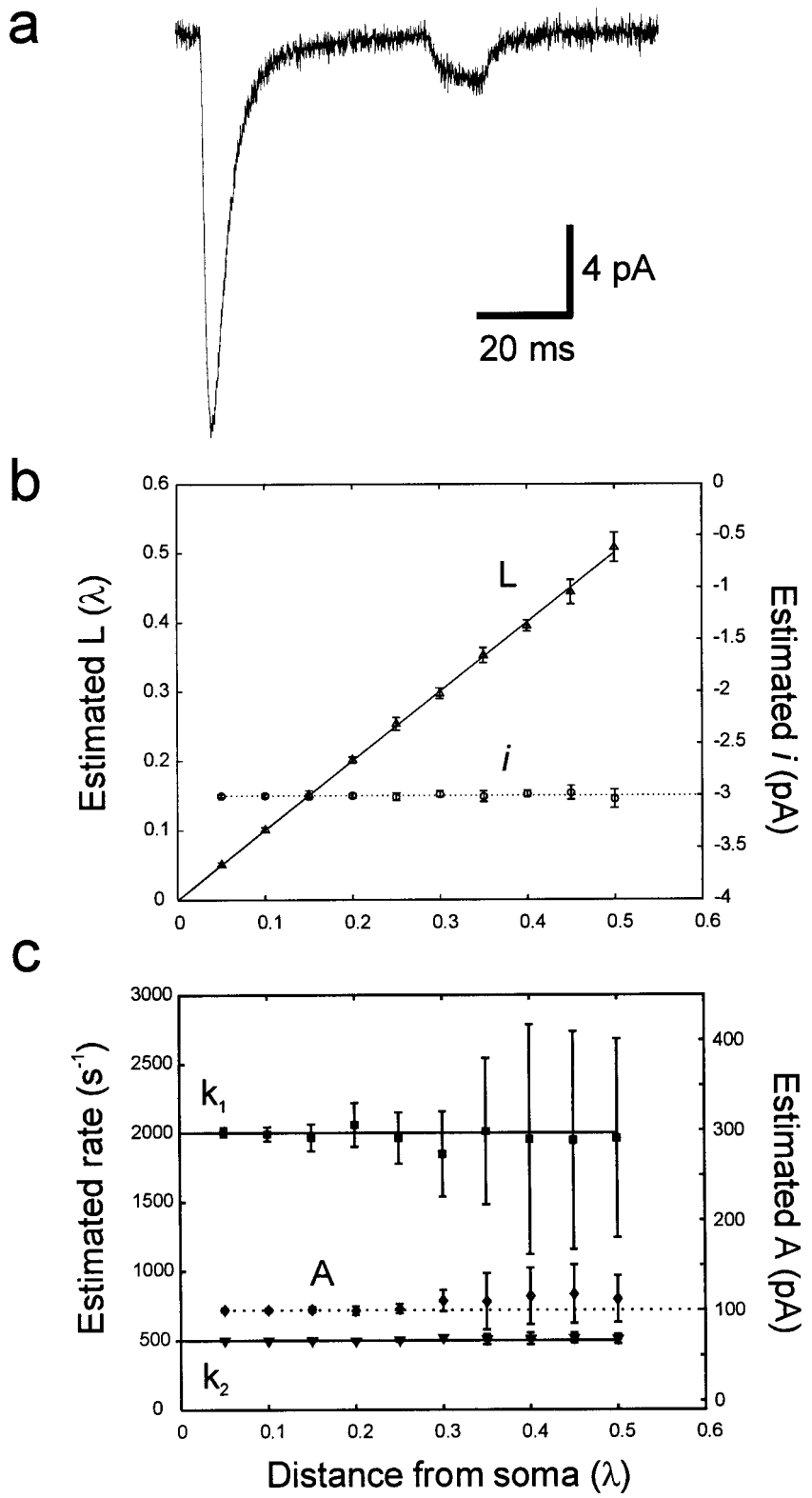

FIGURE 2 Estimating the electrotonic distance and kinetic parameters of synthetic synaptic currents. (*a*) Example synthetic cable-filtered biphasic synaptic current. An AMPA transient was synthesized at $L = 0.15$ according to Eq. 7 with $k_1 = 2000\ s^{-1}$, $k_2 = 500\ s^{-1}$, $A = 100$ pA, and a subsequent NMDA channel opening was synthesized according to Eq. 6, with $i = -3$ pA, and Gaussian baseline noise was added ($\sigma = 0.3$ pA). (*b*) Fitting of single NMDA channel transitions with Eq. 6 estimates L, the distance from synapse to soma. *Circles:* estimated values of i, the single channel current, as a function of L, dotted line indicates actual value. *Triangles:* estimated value of L, solid line indicates actual value. Each point is mean ± SD for 10 channel openings with different segments of baseline noise. τ_m was fixed at its correct value (120 ms), assuming that, in practice, it can be measured independently and accurately. (*c*) Estimated rate constants and amplitude of AMPA phase currents. Values of L from (*b*) were used in fitting AMPA phases with Eq. 7. *Squares:* estimates of k_1; *inverted triangles:* estimates of k_2. Actual values indicated by solid lines. *Diamonds:* estimated value of A, the scaling amplitude of the AMPA phase. Actual value indicated by dotted line. For both (*b*) and (*c*), the initiation times of the events were also free parameters in the fits.

by a dendritic cable from the point of voltage-clamp, behaves virtually as a linear filter. The impulse response of this cable filter may be determined, if single channels can be resolved in the NMDA phase of the synaptic current, using the knowledge that they are essentially perfect step current inputs at the same synaptic site. It was shown how to reconstruct the unfiltered time course of the AMPA transient by deconvolution, and the effects of two types of filter on the AMPA phase were analyzed: a voltage-clamped infinite cable, and a single exponential filter. The simpler

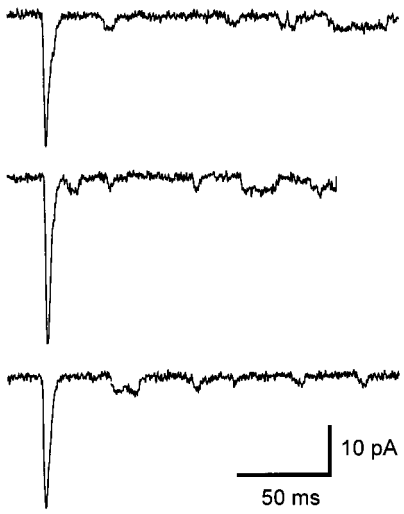

FIGURE 3 Spontaneous biphasic glutamate synaptic currents in cultured rat cortical nonpyramidal neurons, showing a fast AMPA phase, followed by single NMDA channel openings. Filter 1 kHz Gaussian, holding potential −60 mV.

single exponential filter was shown to provide very good fits to the measured AMPA phases in recordings of spontaneous EPSCs in cortical neurons.

The main assumption involved in the recovery of AMPA phase kinetics by deconvolution, as put forward here, is that the transformation between a conductance waveform at the synaptic site and the measured voltage-clamp current at the soma is linear. There is an inherent sublinearity in the current produced by a conductance input as the voltage is deflected toward its reversal potential. However, as shown in Fig. 1 *a*, in a voltage-clamped passive dendrite, with realistic cable parameters, the effect of a current input (assuming perfect clamp at the synaptic site) is, in practice, close to that of a conductance input, and differs detectably only by a linear scaling factor (Fig. 1 *b*). The effect of a voltage-clamped dendrite on an AMPA conductance input, therefore, is accurately modeled as a linear filter. It is highly unlikely that single NMDA channels could even be resolved at electrotonic distances where this assumption would break down.

An aspect that is not captured by the cable model is nonlinearity of the postsynaptic response due to voltage-gated channels activated near the resting potential. The voltage-clamp should confine membrane potential at the synaptic site in a range that is essentially linear over the time scale of the response (e.g., in Fig. 1, peak depolarizations at the synaptic site were only 2.23, 3.82, and 3.84 mV at $\lambda/20$, $\lambda/4$, and $\lambda/2$, respectively). However, such error can be minimized by selecting smaller synaptic currents for analysis and by using intracellular blockers of voltage-dependent current, for example, cesium, to block K currents and QX-314 to block Na-dependent current. These measures would also increase membrane resistance and, therefore, λ.

Another assumption of this technique is that the NMDA receptors activated shortly after an AMPA phase are located

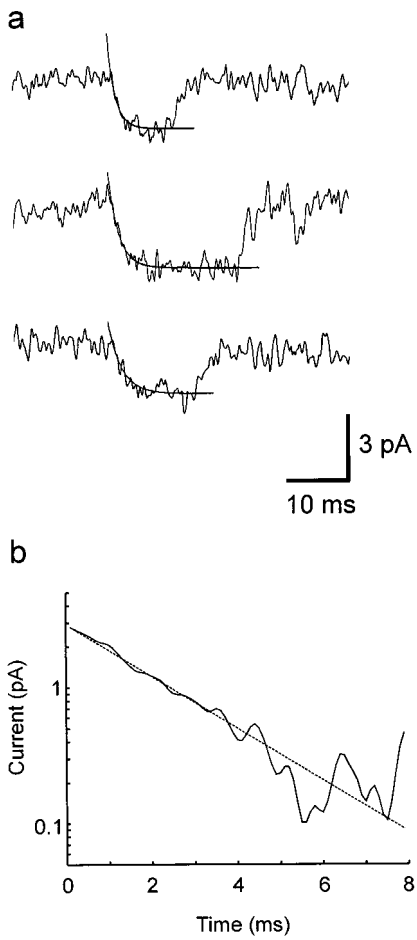

FIGURE 4 Single NMDA channel transitions. (*a*) Three example exponential fits to opening transitions: τ_f values: 1.1 ms (*top*), 1.4 ms (*middle*), 1.4 ms (*bottom*). (*b*) A log-linear plot of the average of 12 NMDA channel openings with τ_f between 2.2 and 2.4 ms (*solid line*), fitted with a time constant of 2.3 ms (*dotted line*).

at the same site as the activated AMPA receptors. Immunocytochemical studies show that NMDA receptors and AMPA receptors are indeed localized at the same synaptic terminals in hippocampus and cortex (He et al., 1998; Kharazia et al., 1996). Miniature spontaneous synaptic currents (in the presence of TTX to block presynaptic action potentials and, presumably, due to release of single presynaptic vesicles) are biphasic (Bekkers and Stevens, 1989, Zhou and Hablitz, 1997), with NMDA and AMPA components. Clearly, like any other approach to estimating AMPA phase kinetics, our technique assumes that a single synaptic locus is activated during each biphasic synaptic event. This condition is most likely to be satisfied by minimally-stimulated or spontaneous miniature synaptic currents, or by intracellular stimulation of single presynaptic cells or terminals. However, if multiple terminals are stimulated precisely in synchrony, the measured time course will be a weighted average of the time courses at the activated sites, provided that the sample of NMDA channel transitions used is selected randomly, so that the number of transitions from

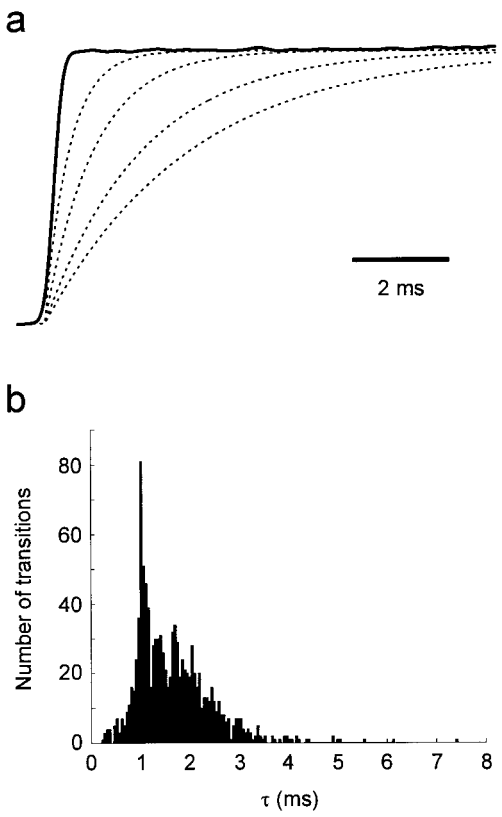

FIGURE 5 Extent of cable filtering of single NMDA channel openings. (*a*) A comparison of the recording system step response (*solid line*) and four single exponential time courses (*dashed lines*), with time constants of 0.5, 1, 2, and 3 ms, within the range of values measured for NMDA channel transitions. The recording system step response was measured as described in the Materials and Methods, and incorporates the effects of a 1-kHz Gaussian digital filter. (*b*) The distribution of time constants of single synaptic NMDA channel transitions measured in one cell.

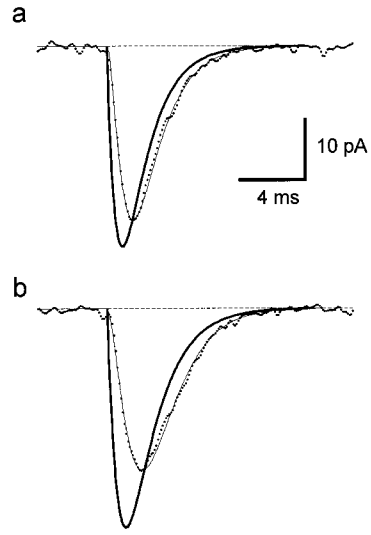

FIGURE 6 Cable-filtered AMPA phases of synaptic currents. Two AMPA phases are shown from the same cell, with different degrees of cable filtering. (*a*) Thin solid line shows fit to Eq. 8 with $\tau_r = 0.6$ ms, $\tau_d = 1.5$ ms, $\tau_f = 0.5$ ms. Thick solid line shows the underlying time course. (*b*) $\tau_r = 0.7$ ms, $\tau_d = 1.7$ ms, $\tau_f = 1$ ms. Holding potential: 60 mV.

each site is in proportion to that site's contribution to the total current.

The main limitation of the present technique is that it requires low-noise recordings, and is therefore more easily applied to small cells, such as granule cells in the cerebellum and nonpyramidal cells in the cortex or hippocampus, or to recordings from dendrites. The main noise source in a typical whole-cell recording comes from the background conductance of the cell membrane. Blocking this tonically or pharmacologically, as described above, will extend the range of cell types that can be examined. However, as this source of noise is reduced, other sources become important. As for all single-channel recordings, care should be taken to minimize pipette capacitance, solution depth, and moisture in the electrode holder, and to use an appropriate headstage circuit.

The technique presented here has several significant advantages over those used previously. The most successful method for measuring the conductance change during fast EPSCs has been to use voltage jumps applied at different times during repeated activation of the synapse (Pearce, 1993), which produce additional ionic current in proportion to the amplitude of the conductance. Variations of this technique have been used in a number of studies (Barbour et al., 1994; Mennerick and Zorumski, 1995; Rossi et al., 1995; Kirson and Yaari, 1996). Häusser & Roth (1997) have shown how measuring the time course of recovered charge during application of voltage steps can give an accurate estimate of the decay time course of the fast conductance. This method can be applied readily to large, leaky cells, and is thus complementary in that sense to our method. Unlike our technique, however, it requires a large ensemble of synaptic conductances acquired under stationary conditions, and is frustrated by quantal variation, plasticity, washout, or other nonstationarities in recording. For practical reasons, it has lower time resolution, and, so far, has been used to measure only the decay phase kinetics and not the rising phase of AMPA receptor-mediated currents. Unlike the voltage-jump method, the present method can be used to recover kinetics of individual events. It can therefore be used to examine variations of AMPA phase timing among large numbers of different synaptic sites in one cell in a straightforward way. This will allow issues such as possible segregation or targeting of receptor subunit types at different locations within cells to be addressed. Measuring individual events will also simplify analysis of the effects of plastic or G-protein receptor-induced changes in AMPA phase kinetics. Another advantage of the present method is that it provides a measure of the cable filter for each synaptic event, in terms of L, the electrotonic distance of the synapse from the site of recording, or, in terms of τ_f, the time constant of the total filtering applied to the synaptic event.

We illustrated the application of this technique using recordings from cultured cortical neurons, and a close com-

parison with values measured from intact cortical tissue is not warranted. Nevertheless, it is worth noting that the average values that we found for the rise and decay time constants (0.4 and 1.5 ms, respectively) are very fast, comparable to those found by Häusser and Roth (1997) in pyramidal neurons of cortical slices, at a temperature approximately 10°C higher. The consistent accuracy of the fits over the entire time course shows that both the difference of two exponentials kinetic model and the single exponential filter are good approximations. It is interesting that, although the Gaussian filtering applied to records has a sigmoid rising phase in its step response, single-channel transitions appeared to follow single exponentials quite well. This can be understood, however, if cable filtering of the form illustrated in Fig. A1 is predominant, because the point of inflexion is very near the beginning of the transients, and may be impossible to resolve in the presence of noise. Furthermore, the curves in Fig. A1 can be fitted fairly well with single exponentials over much of their later time course (not shown).

We speculate that the spread in values measured for rise and decay time constants of synaptic currents reflects some genuine variation in the actual time courses of events, because the fitting error estimated from synthetic data was much smaller. Because we included any well-resolved spontaneous currents, this variation could arise from differences between different synaptic sites as well as differences between successive events at the same site. Such variation could arise, for example, from differences in subunit expression, lipid environment of receptor channels, or time course of glutamate release. Like the NMDA phase, the AMPA phase is composed of stochastic single-channel openings, although of much smaller size and average duration. Some event-to-event deviations of individual currents must also be expected for this reason. A proper examination of these questions, though, will require more extensive data.

In conclusion, we have described a way, which offers some significant advantages over existing strategies, for measuring the true time course and amplitude of the fast excitatory synaptic currents mediated by AMPA receptors. We anticipate that the method will prove useful in understanding how these variables are determined and modulated in mammalian central neurons.

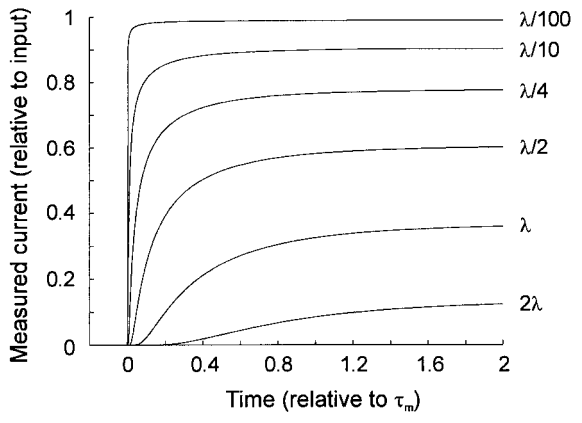

FIGURE A1 The step response of the cable filter at different synaptic distances. Eq. 6 is plotted for different values of L, as indicated at the right. Opening and closing transitions of single NMDA channels would be expected to follow this form.

APPENDIX A. CABLE FILTERING IN A VOLTAGE-CLAMPED INFINITE UNIFORM CABLE

In this section, we derive the expected cable filter characteristic for a dendrite, modeled as a semi-infinite cable with a perfect voltage-clamp applied at the soma. The voltage response of an infinite cylindrical cable to a delta pulse of charge Q_0, applied at $T = 0$ and $X = 0$, is given by

$$V_\delta = \frac{Q_0}{2c_m\lambda\sqrt{\pi T}}\exp\left(\frac{-X^2 - 4T^2}{4T}\right), \tag{A1}$$

where λ is the space constant, T is the time in units of the time constant, X is the distance in units of the space constant and c_m is the membrane capacitance per unit-length of cable (Eq. 3.48 of Jack et al., 1983, p. 46). Let the soma be at a distance L from the site of current injection. Applying a perfect voltage-clamp to a potential of 0 (the resting potential) at the soma is equivalent to injecting simultaneously a reflection charge of $-Q_0$ at a distance of $2L$. Thus, at $X = L$, the sum of the responses is always zero—the voltage is clamped to zero. The voltage impulse response of the infinite cable with a voltage-clamp at $X = 0$ is therefore

$$V_\delta = \frac{Q_0}{2c_m\lambda\sqrt{\pi T}}\left[\exp\left(\frac{-X^2 - 4T^2}{4T}\right) - \exp\left(\frac{-(2L - X)^2 - 4T^2}{4T}\right)\right]. \tag{A2}$$

The axial current flowing in the cable is given by

$$I(T) = -\left(\frac{1}{r_a\lambda}\right)\frac{\partial V}{\partial X}. \tag{A3}$$

Evaluating this spatial derivative at $X = L$ gives the axial current at the site of the voltage-clamp, which is the current measured by the voltage-clamp (Eq. 5)

$$I(T) = \frac{Q_0 L\exp[(-L^2 - 4T^2)/4T]}{2\tau_m\sqrt{\pi}T^{3/2}}, \tag{A4}$$

where τ_m is the membrane time constant. The Laplace transform of this cable filter impulse response can be derived as follows. The right-hand side can be rewritten as the product of three terms,

$$\frac{Q_0}{2\tau_m\sqrt{\pi}}\cdot\frac{L\exp(-L^2/4T)}{T^{3/2}}\cdot\exp(-T). \tag{A5}$$

The first term is simply a constant. The Laplace transform of the second term is $2\sqrt{\pi}\exp(-L\sqrt{s})$ (transform pair 3.2.7 of Roberts and Kaufman, 1966, p. 22). Since, if $g(s)$ is the Laplace transform of $f(T)$, then $g(s + 1)$ is the Laplace transform of $f(T)\exp(-T)$, the Laplace transform of Eq. A4 is given by

$$\bar{I}(s) = \frac{Q_0}{\tau_m}\exp(-L\sqrt{s + 1}). \tag{A6}$$

This can be readily used to calculate expressions for the convolution of a given dendritic current input with Eq. A4 by multiplying with the Laplace transform of the input current waveform, and taking the inverse Laplace transform. We will use this approach below, when calculating an expres-

sion for the expected voltage-clamp current, with a synaptic current following a 2-exponential time course.

The step response of this cable filter should be used to fit the shape of single-channel opening and closing transitions in a voltage-clamped infinite dendrite. It can be found using the Laplace transform method or the reflection method, which we give here.

The voltage response of an infinite cable to a step function of current of size I_0, applied at time zero, is

$$V_{\text{step}} = \frac{r_a I_0 \lambda}{4}\left\{\exp(-X)\text{erfc}\left(\frac{X}{2\sqrt{T}} - \sqrt{T}\right) - \exp(X)\text{erfc}\left(\frac{X}{2\sqrt{T}} + \sqrt{T}\right)\right\} \tag{A7}$$

(Eq. 3.24 of Jack et al., 1983, p. 30). To apply voltage clamp at a distance L, the reflection response to an image current at $2L$ is subtracted,

$$V_{\text{step}} = \frac{r_a I_0 \lambda}{4}\left\{\begin{aligned}&\exp(-X)\text{erfc}\left(\frac{X}{2\sqrt{T}} - \sqrt{T}\right)\\ &\quad - \exp(X)\text{erfc}\left(\frac{X}{2\sqrt{T}} + \sqrt{T}\right)\\ &- \exp(-2L + X)\text{erfc}\left(\frac{2L - X}{2\sqrt{T}}\right)\\ &\quad + \exp(2L - X)\text{erfc}\left(\frac{2L - X}{2\sqrt{T}} + \sqrt{T}\right)\end{aligned}\right\}. \tag{A8}$$

As above, for the impulse response, the voltage-clamp current is the first spatial derivative of this, evaluated at $X = L$ (Eq. 6),

$$I(T) = \frac{I_0}{2}\left\{e^{-L} + e^{-L}\text{erf}\left(\frac{2T - L}{2\sqrt{T}}\right) + e^{L}\text{erfc}\left(\frac{2T + L}{2\sqrt{T}}\right)\right\}. \tag{A9}$$

This step response is plotted for several different distances along the dendrite in Figure A1.

The difference of two exponentials description of the underlying synaptic current (Eq. 4) has the Laplace transform,

$$\bar{I}(s) = A\left[\frac{1}{s + k_2} - \frac{1}{s + k_1}\right]. \tag{A10}$$

The observed voltage-clamp current at the soma in response to an AMPA conductance transient in the dendrite, is the convolution of Eqs. 4 and A4, evaluated by taking the inverse transform of the product of Eqs. A6 and A10. This gives the solution,

$$I(T) = \frac{LA}{2\sqrt{\pi}}\int_0^T \frac{\exp(k_1 u - k_1 T) - \exp(k_2 u - k_2 T)}{u^{3/2}\exp(u + (L^2/4u))}\text{d}u. \tag{A11}$$

To demonstrate the correctness of this equation, it is plotted in Fig. A2 for two different distances along the dendrite, superimposed on the corresponding solutions from the numerical model used in Fig. 1.

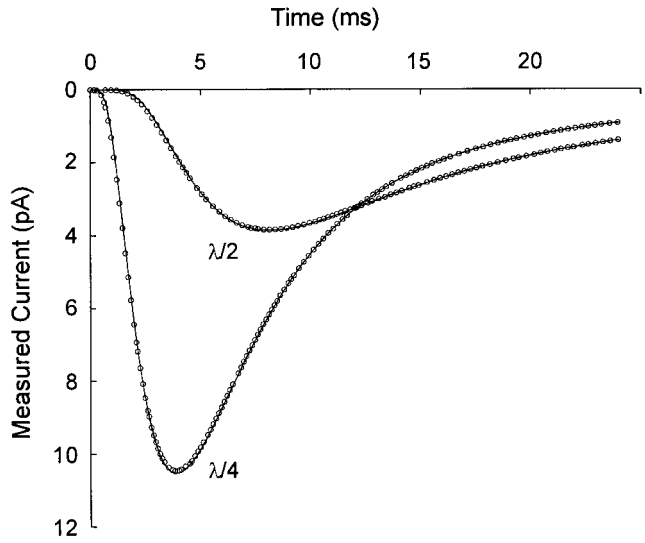

FIGURE A2 Correspondence between analytical theory and compartmental model. Voltage-clamped AMPA phase currents, with parameters as in Fig. 1, are calculated in a compartmental model at two different distances from the voltage-clamp, λ/4 and λ/2 (*circles*), and superimposed on the corresponding curves given by Eq. 7.

APPENDIX B. EXPONENTIAL FILTERING OF SYNAPTIC CURRENTS

Here, we derive an expression for the observed current waveform for a simple model of filtering of synaptic currents, which lumps together cable and apparatus filtering into a single-exponential filter. The exponential filter has a Laplace transform,

$$F(s) = \frac{D}{\tau_f(s + 1/\tau_f)}, \tag{B1}$$

where D is the ratio of the measured single-channel current amplitude to the actual value (i.e., the scale of the filter). Therefore, the Laplace transform of the observed AMPA phase is given by the product of Eqs. A10 and B1,

$$\bar{I}(s) = \frac{AD[1/(s + 1/\tau_d) - 1/(s + 1/\tau_r)]}{\tau_f(s + 1/\tau_f)}, \tag{B2}$$

where $\tau_d = 1/k_2$ and $\tau_r = 1/k_1$. The inverse Laplace transform of this is the observed time course of the AMPA phase,

$$I(t) = AD\left[\frac{\tau_d\exp(-t/\tau_d)}{\tau_d - \tau_f} - \frac{\tau_r\exp(-t/\tau_r)}{\tau_r - \tau_f} + \frac{\tau_f(\tau_d - \tau_r)\exp(-t/\tau_f)}{(\tau_f - \tau_d)(\tau_f - \tau_r)}\right]. \tag{B3}$$

For mathematical completeness, we give the limits of Eq. B3 for $\tau_f \to \tau_r$ or $\tau_f \to \tau_d$, when Eq. B3 is indeterminate:

$$\lim_{\tau_f \to \tau_r} I(t) = \frac{AD}{\tau_r(\tau_d - \tau_r)}\exp\left(\frac{-t(\tau_r + \tau_d)}{\tau_d\tau_r}\right) \times [\tau_d\tau_r(e^{t/\tau_r} - e^{t/\tau_d}) + te^{t/\tau_d}(\tau_r - \tau_d)] \tag{B4}$$

$$\lim_{\tau_f \to \tau_d} I(t) = \frac{AD}{\tau_d(\tau_d - \tau_r)}\exp\left(\frac{-t(\tau_r + \tau_d)}{\tau_d\tau_r}\right) \times [\tau_d\tau_r(e^{t/\tau_d} - e^{t/\tau_r}) + te^{t/\tau_r}(\tau_d - \tau_r)]. \tag{B5}$$

We thank Dr. Mikko Juusola for helpful discussions. This work was supported by grants from the Human Frontiers Science Program (RG 89/94B) and the European Community Biotech Programme (CT960211). I. C. K. was supported by the Deutsche Akadimischer Austauschdienst and the Studientstiftung des Deutschen Volkes.

REFERENCES

Barbour, B., B. U. Keller, I. Llano, and A. Marty. 1994. Prolonged presence of glutamate during excitatory synaptic transmission to cerebellar Purkinje cells. *Neuron.* 12:1331–1343.

Bekkers, J. M., and C. F. Stevens. 1989. NMDA and non-NMDA receptors are colocalized at individual excitatory synapses in cultured rat hippocampus. *Nature.* 341:230–233.

Carnevale, N. T., and D. Johnston. 1982. Electrophysiological characterization of remote chemical synapses. *J. Neurophysiol.* 47:606–621.

Colquhoun, D., P. Jonas, and B. Sakmann. 1992. Action of brief pulses of glutamate on AMPA and kainate receptors in patches from different neurons of rat hippocampal slices. *J. Physiol.* 458:261–287.

Colquhoun, D., and F. J. Sigworth. 1995. Fitting and statistical analysis of single-channel records. *In* Single Channel Recording. B. Sakmann and E. Neher, editors. Plenum Press, New York. 483–587.

Forsythe, I. D., and M. Barnes-Davies. 1993. The binaural auditory pathway—excitatory amino-acid receptors mediate dual timecourse excitatory postsynaptic currents in the rat medial nucleus of the trapezoid body. *Proc. R. Soc. Lond. (Biol.).* 251:151–157.

Forsythe, I. D., and G. L. Westbrook. 1988. Slow excitatory postsynaptic currents mediated by *N*-methyl-D-aspartate receptors on cultured mouse central neurones. *J. Physiol.* 396:515–533.

Häusser, M. 1994. Kinetics of excitatory synaptic currents in Purkinje cells studied using dendritic patch-clamp recording. *Soc. Neurosci. Abstr.* 20:891.

Häusser, M., and A. Roth. 1997. Estimating the time course of the excitatory synaptic conductance in neocortical pyramidal cells using a novel voltage jump method. *J. Neurosci.* 17:7606–7625.

He, Y., W. G. M. Janssen, and J. H. Morrison. 1998. Synaptic coexistence of AMPA and NMDA receptors in the rat hippocampus: a postembedding immunogold study. *J. Neurosci. Res.* 54:444–449.

Hestrin, S. 1993. Different glutamate receptor channels mediate fast excitatory synaptic currents in inhibitory and excitatory cortical neurons. *Neuron.* 11:1083–1091.

Hille, B. 1992. Ionic Channels of Excitable Membranes. Sinauer, Sunderland, MA.

Hollmann, M., and S. Heinemann. 1994. Cloned glutamate receptors. *Ann. Rev. Neurosci.* 17:31–108.

Jack, J. J. B., D. Noble, and R. W. Tsien. 1983. Electric Current Flow in Excitable Cells. Paperback Edition, Oxford University Press, Oxford.

Jackson, M. B. 1992. Cable analysis with the whole-cell patch clamp—theory and experiment. *Biophys. J.* 61:756–766.

Johnston, D., and T. H. Brown. 1983. Intrepretation of voltage-clamp measurements in hippocampal neurons. *J. Neurophysiol.* 50:464–486.

Jonas, P., C. Racca, B. Sakmann, P. H. Seeburg, and H. Monyer. 1994. Differences in Ca^{2+} permeability of AMPA-type glutamate receptor channels in neocortical neurons caused by differential GluR-B subunit expression. *Neuron.* 12:1281–1289.

Kharazia, V. N., and R. J. Weinberg. 1997. Tangential synaptic distribution of NMDA and AMPA receptors in rat neocortex. *Neurosci. Lett.* 238: 41–44.

Kirson, E. D., and Y. Yaari. 1996. Synaptic NMDA receptors in developing mouse hippocampal neurones: functional properties and sensitivity to ifenprodil. *J. Physiol. (Lond.).* 497:437–455.

Maeda, E., H. P. C. Robinson, and A. Kawana. 1995. The mechanisms of generation and propagation of synchronized bursting in developing networks of cortical neurons. *J. Neurosci.* 15:6834–6845.

Major, G., A. U. Larkman, P. Jonas, B. Sakmann, and J. J. B. Jack. 1994. Detailed passive cable models of whole-cell recorded CA3 pyramidal neurons in rat hippocampal slices. *J. Neurosci.* 14:4613–4638.

Mennerick, S., and C. F. Zorumski. 1995. Presynaptic influence on the time course of fast excitatory synaptic currents in cultured hippocampal cells. *J. Neurosci.* 15:3178–3192.

Nowak, L., P. Bregestovski, P. Ascher, A. Herbet, and A. Prochiantz. 1984. Magnesium gates glutamate-activated channels in mouse central neurones. *Nature.* 307:462–465.

Ozawa, S., H. Kamiya, and K. Tsuzuki. 1998. Glutamate receptors in the mammalian central nervous system. *Prog. Neurobiol.* 54:581–618.

Pearce, R. A. 1993. Physiological evidence for two distinct GABA responses in rat hippocampus. *Neuron.* 10:189–200.

Rall, W. 1969. Time constants and electrotonic length of membrane cylinders and neurons. *Biophys. J.* 9:1483–1508.

Roberts, G. E., and H. Kaufman. 1966. Table of Laplace Transforms. W.B. Saunders, Philadelphia and London.

Robinson, H. P. C., Y. Sahara, and N. Kawai. 1991. Nonstationary fluctuation analysis and direct resolution of single channel currents at postsynaptic sites. *Biophys. J.* 59:295–304.

Rossi, D. J., S. Alford, E. Mugnaini, and N. T. Slater. 1995. Properties of transmission at a giant glutamatergic synapse in cerebellum: the mossy fiber-unipolar brush cell synapse. *J. Neurophysiol.* 74:24–42.

Sigworth, F. J. 1986. Open channel noise. II. A test for coupling between current fluctuations and conformational transitions in the acetylcholine receptor. *Biophys. J.* 49:1041–1046.

Silver, R. A., S. F. Traynelis, and S. G. Cull-Candy. 1992. Rapid-time-course miniature and evoked excitatory currents at cerebellar synapses *in situ.* Nature. 355:163–166.

Silver, R. A., M. Farrant, and S. G. Cull-Candy. 1995. Filtering of the synaptic current estimated from the time course of NMDA channel opening. *Soc. Neurosci. Abstr.* 21:584.

Spruston, N., D. B. Jaffe, S. H. Williams, and D. Johnston. 1993. Voltage- and space-clamp errors associated with the measurement of electrotonically remote synaptic events. *J. Neurophysiol.* 70:781–802.

Stern, P., F. A. Edwards, and B. Sakmann. 1992. Fast and slow components of unitary EPSCs on stellate cells elicited by focal stimulation in slices of rat visual cortex. *J. Physiol.* 449:247–278.

Zhou, F. M., and J. J. Hablitz. 1997. Rapid kinetics and inward rectification of miniature EPSCs in layer I neurons of rat neocortex. *J. Neurophysiol.* 77:2416–2426.